

# Large-scale Analysis of *in Vivo* Phosphorylated Membrane Proteins by Immobilized Metal Ion Affinity Chromatography and Mass Spectrometry\*

Thomas S. Nühse‡, Allan Stensballe§, Ole N. Jensen§¶, and Scott C. Peck‡¶

Global analyses of protein phosphorylation require specific enrichment methods because of the typically low abundance of phosphoproteins. To date, immobilized metal ion affinity chromatography (IMAC) for phosphopeptides has shown great promise for large-scale studies, but has a reputation for poor specificity. We investigated the potential of IMAC in combination with capillary liquid chromatography coupled to tandem mass spectrometry for the identification of plasma membrane phosphoproteins of *Arabidopsis*. Without chemical modification of peptides, over 75% pure phosphopeptides were isolated from plasma membrane digests and detected and sequenced by mass spectrometry. We present a scheme for two-dimensional peptide separation using strong anion exchange chromatography prior to IMAC that both decreases the complexity of IMAC-purified phosphopeptides and yields a far greater coverage of monophosphorylated peptides. Among the identified sequences, six originated from different isoforms of the plasma membrane H<sup>+</sup>-ATPase and defined two previously unknown phosphorylation sites at the regulatory C terminus. The potential for large-scale identification of phosphorylation sites on plasma membrane proteins will have wide-ranging implications for research in signal transduction, cell-cell communication, and membrane transport processes. *Molecular & Cellular Proteomics* 2: 1234–1243, 2003.

Signal transduction pathways have traditionally been elucidated by identifying receptors, kinases, and substrates one by one and individually establishing the connections between them. In recent years, new mass spectrometric techniques and instrumentation have revolutionized our ability to analyze the cellular proteome on a large scale, and a global analysis of all phosphorylated proteins (and ultimately the dynamics of phosphorylation) appears to be within reach. Although a large

percentage of cellular proteins can be phosphorylated (1, 2), the abundance of the individual phosphorylated forms is frequently low. Without specific enrichment, only the most abundant phosphoproteins would be identified. At the level of full-length proteins, mostly tyrosine-phosphorylated proteins have been successfully enriched by immunoprecipitation (3–5), although the approach is feasible in principle with serine- and threonine-phosphorylated proteins (6). Enrichment strategies on the level of phosphopeptides have the advantage of identifying both the protein and the phosphorylated residues, which is otherwise a challenging task. Specific capture of phosphopeptides is possible by  $\beta$ -elimination of the phosphate group and subsequent introduction of an affinity tag (7), by covalent capture and release (8), or by affinity chromatography with immobilized metal ions (IMAC)<sup>1</sup> (9–13). The former two methods have been designed for enhanced specificity but involve complex chemistry and have therefore not been widely used. The simpler IMAC technique has been used in several medium- and large-scale phosphoproteomic studies as well as in several phosphorylation site identifications on single proteins (14).

We are interested in the signal transduction processes triggered in plant cells by the perception of microbial elicitors of defense responses. Plasma membrane proteins are involved in the perception of elicitors, in regulating early responses, and are targets of bacterial virulence factors (15–20). The identification of signaling processes and phosphoproteins at the plasma membrane is thus of great interest. Specific changes in protein phosphorylation can be visualized by *in vivo* pulse labeling with [<sup>33</sup>P] orthophosphate and the differentially phosphorylated proteins identified by two-dimensional PAGE and nano-electrospray ionization tandem mass spectrometry (MS/MS) (21). We applied this functional proteomic approach to plasma membranes of *in vivo*-labeled cells and identified two intrinsic membrane proteins with al-

From ‡The Sainsbury Laboratory, John Innes Centre, Colney Lane, Norwich NR4 7UH, United Kingdom, and §Department of Biochemistry and Molecular Biology, University of Southern Denmark, DK-5230 Odense M, Denmark

Received, May 19, 2003, and in revised form, September 18, 2003  
Published, MCP Papers in Press, September 22, 2003, DOI 10.1074/mcp.T300006-MCP200

<sup>1</sup> The abbreviations used are: IMAC, immobilized metal ion affinity chromatography; MS/MS, tandem mass spectrometry; LC, liquid chromatography; NTA, nitrilotriacetic acid; DTT, dithiothreitol; SAX, strong anion exchange; MALDI, matrix-assisted laser desorption/ionization; Q-TOF, quadrupole time-of-flight; TLC, thin-layer chromatography; TLE, thin-layer electrophoresis; IDA, iminodiacetic acid; SCX, strong cation exchange.

tered phosphorylation levels in response to elicitors.<sup>2</sup> The number of phosphoproteins, however, was substantially lower than observed using one-dimensional SDS-PAGE, and it appears that the method is not effective for membrane proteins with more than one transmembrane helix. Thus, we sought alternative methods for analyzing these proteins.

The problem of membrane protein insolubility can be circumvented by proteolytic digestion of the intact membranes and analysis of peptides released from extramembrane domains (22). This approach has been used for large-scale "shotgun" proteomics of membrane proteins (23, 24) as well as the analysis of phosphorylation sites on thylakoid proteins (11). Here, we demonstrate that the combination of trypsin digestion of cytoplasmic face-out vesicles, IMAC and liquid chromatography (LC)-MS/MS is a suitable strategy for large-scale phosphoproteomics of the plasma membrane. Contrary to a common misconception, we found the specificity of IMAC for phosphopeptides to be good, and we present a novel two-dimensional separation strategy that yields greater coverage especially of monophosphorylated peptides.

#### MATERIALS AND METHODS

**Materials**—All chemicals, unless otherwise stated, were obtained from Sigma or Fluka.  $\alpha$ -Cyanohydroxycinnamic acid was recrystallized from acetonitrile prior to use. Scandium (III) nitrate and gallium (III) nitrate were purchased from Aldrich (Gillingham, UK). Flagellin peptide (flg22) was synthesized by Affiniti Research Products (Mamhead, UK). Radioisotopes and dextran T-500 were purchased from Amersham Biosciences (Chalfont St Giles, UK); modified porcine trypsin was purchased from Promega (Southampton, UK); POROS® chromatography materials (Self Pack OligoR3, MC 20, HQ 20) were purchased from Applied Biosystems (Foster City, CA); thin-layer chromatography plates were obtained from Merck (Darmstadt, Germany); nitrilotriacetic acid (NTA)-silica and NTA-agarose were obtained from Qiagen (Crawley, UK); and immobilized alkaline phosphatase was obtained from MoBiTec (Göttingen, Germany). Microcolumns were packed in Gelloader tips as described in (25).

**Cell Culture, Elicitor Treatment, and *in Vivo* Labeling**—Suspension-cell cultures of *Arabidopsis thaliana* ecotype Landsberg (26) were used 7 days after subculturing 1 ml into 100 ml. Flagellin peptide (flg22) (27) was used at a concentration of 100 nM. The cells were treated with the peptide for 4 min prior to labeling with 20–40 MBq [<sup>32</sup>P]orthophosphate, as described in (28).

**Cell Fractionation**—Suspension-cultured cells were collected by filtration and resuspended in ice-cold homogenization buffer (250 mM sucrose, 100 mM HEPES/KOH, pH 7.5, 10 mM EDTA, 5% glycerol, 0.5% polyvinylpyrrolidone K 25, 3 mM dithiothreitol (DTT), 1 mM phenylmethylsulfonyl fluoride; with addition of 50 mM sodium pyrophosphate, 25 mM sodium fluoride, and 1 mM sodium molybdate for phosphoprotein analysis) at 2 ml/g fresh weight. The slurry was enclosed in a Parr bomb (Parr Instruments, Moline, IL) and stirred for 45 min at 4 °C after addition of nitrogen gas to a pressure of 70 bar/1000 psi. Cells were broken by release of the pressure, and the homogenate was centrifuged for 10 min at 1500 × *g* (GSA rotor, 3500 rmin<sup>-1</sup>). The supernatant was centrifuged for 30 min at 120,000 × *g* (Ti 45 rotor, 33,000 rmin<sup>-1</sup>) to yield a microsomal fraction. For plasma membrane purification, the microsomal pellets were resuspended in buffer R (250 mM sucrose, 5 mM potassium phosphate, pH 7.5, 6 mM

KCl) and subjected to phase partitioning (29) in 6.0% each dextran T-500 and polyethylene glycol 3350 in buffer R. The U3 phase was diluted ca. 5-fold with buffer R, and plasma membranes were harvested by centrifugation for 60 min at 150,000 × *g*.

For homogenization of *in vivo*-labeled cells, the homogenization buffer was supplemented with 5 μM leupeptin, 1 μM K252a, and 100 nM calyculin A. Cells were broken in a potter homogenizer on ice, and cell debris was pelleted by centrifugation at 3000 × *g* for 5 min. The supernatant was removed and centrifuged at 120,000 × *g* for 30 min at 4 °C. The microsomal pellets were resuspended in a small volume of buffer R and added to a complete phase mix with microsomes from a large nonradioactive preparation, and the phase separation was performed as described above.

**Proton Pumping Assay**—The assay was done as described in (30). Briefly, 50 mg of plasma membrane protein were diluted into 1 ml assay buffer (20 μM acridine orange, 10 mM 4-morpholinepropane-sulfonic acid-bis-Tris propane, pH 7.0, 140 mM KCl, 4 mM MgCl<sub>2</sub>, 1 mM EDTA, 1 mM DTT, 1 mg/ml bovine serum albumin) containing the indicated concentrations of Brij-58 (0–0.02%). The reaction was started by adding ATP to a final concentration of 2 mM, and the decrease in absorbance at 495 nm was measured in a spectrophotometer. The establishment of a proton gradient was verified by the addition of 1 μg/ml nigericin, which immediately destroyed the gradient.

**Trypsin Treatment of Plasma Membranes**—Plasma membrane pellets were carbonate-washed by resuspension in a small volume of buffer R plus 0.02% Brij-58 and 10-fold dilution in 100 mM ice-cold Na<sub>2</sub>CO<sub>3</sub>. After incubation on ice for 15 min with occasional vortexing, the membranes were harvested by centrifugation (30 min at 100,000 × *g*). Two more washes with 500 mM and 50 mM NH<sub>4</sub>HCO<sub>3</sub> were performed before resuspending the pellet in a minimal volume of 50 mM NH<sub>4</sub>HCO<sub>3</sub> for overnight trypsin digestion (1 μg trypsin per 50 μg protein) at 37 °C. The supernatant containing the released peptides was either used directly for IMAC after addition of 0.2 M acetic acid (see Fig. 3), or 5% formic acid was added to the digest and the supernatant purified over an R3 column as described below for quantitative experiments and prior to strong anion exchange (SAX) chromatography.

**Two-dimensional Phosphopeptide Analysis**—The released phosphopeptides were separated from the membrane by ultracentrifugation (1 h at 200,000 × *g*), dried in a speedvac, and several times redissolved in water and dried again to remove the ammonium salt. After dissolving in 0.1 M acetic acid, the peptides were applied onto a pre-equilibrated Fe<sup>3+</sup>-NTA column (31), washed with four volumes of 0.1 M acetic acid and two volumes of water, and eluted with dilute ammonia, pH 10. Eluate fractions with the highest Cerenkov counting were pooled, dried, and analyzed by thin-layer chromatography/electrophoresis as described (32), using a pH 8.9 buffer for the electrophoresis dimension.

**Immobilized Metal Ion Affinity Chromatography**—IMAC resins were pretreated according to the manufacturer's instructions for POROS MC material. Chromatography was performed as described in (12) with minor modifications. Peptides were batch-bound to the IMAC material by shaking at room temperature in a typical volume of 20–50 μl, containing ca. 2–5 μl (settled volume) of IMAC material. No significant difference in phosphopeptide recovery (as measured with radiolabeled peptides) was observed with incubation times between 5 and 60 min (data not shown). After the incubation, the slurry was packed into Gelloader® pipette tips with constricted tips and washed once each with 15 μl 0.1 M acetic acid and 0.1 M acetic acid/30% acetonitrile, respectively, before elution with dilute ammonia, pH 10.5, or 50 mM ammonium phosphate, pH 9. Complete elution of phosphopeptides was achieved with 10 μl (as tested with radiolabeled peptides, see below) if the resin was equilibrated with eluting buffer (3 μl) and incubated for 5–10 min before eluting with the remaining (7 μl) buffer.

<sup>2</sup> T. S. Nühse, T. Boller, and S.C. Peck, submitted for publication.

**Quantitation of IMAC Efficiency with Radiolabeled Peptides**—Ca. 500  $\mu\text{g}$  of microsomal protein (prepared as described in “Cell Fractionation”) were washed in kinase buffer (50 mM HEPES-KOH, pH 7.5, 10 mM  $\text{MgCl}_2$ , 1 mM DTT, 10  $\mu\text{M}$   $\text{CaCl}_2$ ) and autophosphorylated with 1 MBq [ $\gamma$ - $^{32}\text{P}$ ]-ATP (50  $\mu\text{M}$  total ATP) for 1 h. Ten volumes of 8 M urea were added, and membranes were recovered by centrifugation (10 min at  $20,000 \times g$ ). After two more washes with urea and one wash with 0.1 M  $\text{NH}_4\text{HCO}_3$ /10 mM DTT, 20  $\mu\text{g}$  trypsin in 50 mM  $\text{NH}_4\text{HCO}_3$  were added, and the membranes were digested overnight at 37 °C with shaking. Formic acid was added to a concentration of 5%, and after centrifugation (20 min at  $20,000 \times g$ ), peptides were recovered from the supernatant by purification over a microcolumn with POROS R3. The peptides were eluted from the R3 material with 0.1 M acetic acid/50% acetonitrile, diluted with 0.1 M acetic acid, and used in IMAC assays as described above. For quantification, aliquots of the labeled peptides (equal to the amount used for IMAC) were spotted onto small filter papers and dried. Likewise, unbound material (including washes) and eluates were spotted on filters for quantification. Radioactivity was measured by PhosphorImaging.

**Mass Spectrometry**—Matrix-assisted laser desorption/ionization (MALDI) spectra of phosphopeptides were acquired by desalting the IMAC eluates on an R3 microcolumn and eluted directly onto the target plate with saturated 2,5-dihydroxybenzoic acid in 50% acetonitrile. For dephosphorylation, phosphopeptides were eluted from R3 with 50% acetonitrile, diluted into phosphatase buffer (supplied with the immobilized enzyme), and slowly passed over a microcolumn of immobilized alkaline phosphatase. The eluate was desalted on an R3 microcolumn and eluted onto the target with saturated  $\alpha$ -hydroxycinnamic acid in 50% acetonitrile/2.5% formic acid. MALDI spectra were acquired on a Bruker Reflex IV (Bruker, Billerica, MA).

Automated nanoflow LC-MS/MS analysis was performed using a quadrupole time-of-flight (Q-TOF) Ultima mass spectrometer (Waters/Micromass UK Ltd., Manchester, UK) employing automated data-dependent acquisition. A nanoflow high-pressure LC system (Ultimate; Switchos2; Famos; LC Packings, Amsterdam, The Netherlands) was used to deliver a flow rate of  $175 \text{ nl min}^{-1}$  to the mass spectrometer. Chromatographic separation was accomplished by using a 2-cm fused silica precolumn (75  $\mu\text{m}$  inner diameter; 360  $\mu\text{m}$  outer diameter; Zorbax® SB-C18 5  $\mu\text{m}$  (Agilent, Wilmington, DE)) connected to an 8-cm analytical column (50  $\mu\text{m}$  inner diameter; 360  $\mu\text{m}$  outer diameter; Agilent Zorbax® SB-C18 3.5  $\mu\text{m}$ ). Peptides were eluted by a gradient of 5–32% acetonitrile in 35 min.

The mass spectrometer was operated in positive ion mode with a source temperature of 80 °C and a countercurrent gas flow rate of 150 liters  $\text{h}^{-1}$ . Data-dependent analysis was employed (three most abundant ions in each cycle): 1 s MS  $m/z$  350–1500 and max 4 s MS/MS  $m/z$  50–2000 (continuum mode), 30 s dynamic exclusion.

Raw data were processed using MassLynx 3.5 ProteinLynx (smooth 3/2 Savitzky Golay and center 4 channels/80% centroid), and the resulting MS/MS dataset was exported in the Micromass pkl format. We performed the peptide identification and assignment of partial post-translational modifications using an in-house version of Mascot v. 1.9. All datasets were searched twice, first with relatively large peptide mass tolerances, followed by internal mass recalibration by an in-house software algorithm using theoretical masses from unambiguously identified peptides obtained from the first search. The recalibrated datasets were searched against NCBItr (all species) using the following constraints: only tryptic peptides with up to three missed cleavage sites were allowed; 0.1 Da mass tolerances for MS and MS/MS fragment ions. Phosphorylation (STY), deamidation (NQ), and oxidation (M) were specified as variable modifications. The results were filtered for non-*Arabidopsis* peptide assignments, and a large number of assigned phosphopeptides were verified manually by either assignment of phosphorylation sites or presence of neutral loss

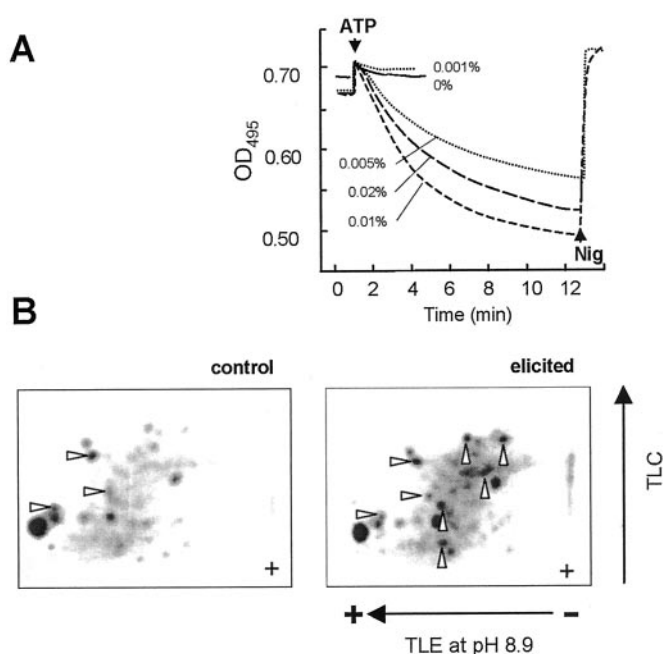


**FIG. 1. Inversion of plant plasma membrane vesicles for the recovery of phosphopeptides from the cytoplasmic face.** A, low concentrations of the detergent Brij-58 generate sealed inside-out vesicles, as visualized by ATP-dependent proton pumping activity in Brij-58-pretreated plasma membrane vesicles. The decrease in absorption of acridine orange reflects the acidification of the vesicle lumen. Addition of 1  $\mu\text{M}$  nigericin (Nig) abolishes the established pH gradient. B, two-dimensional TLC/TLE of phosphopeptides from *in vivo*-labeled plasma membranes that have been inverted with Brij-58 and “shaved” with trypsin. The origin (site of sample application) is indicated by “+.” Signals that are strongly induced in elicited versus control samples are marked with upward pointing arrowheads, unchanged signals (showing even loading) with arrowheads pointing right.

of phosphoric acid during collision-induced dissociation. External mass calibration using NaI resulted generally in mass errors of less than 50 ppm, typically 5–15 ppm in the  $m/z$  range 50–2000.

**Two-dimensional LC**—Plasma membranes (500  $\mu\text{g}$ ) were trypsin-digested, and the released peptides were purified over an R3 microcolumn as described for quantitative IMAC, but washed with water before elution with 50% acetonitrile. The eluate was diluted with buffer and pH-adjusted to final concentrations of 30% acetonitrile/20 mM  $\text{NH}_4\text{HCO}_3$ , pH  $\sim 7$ . A microcolumn was packed with POROS SAX and pre-equilibrated with 30% acetonitrile/25 mM  $\text{NH}_4\text{HCO}_3$ , pH 7 (SAX buffer). The sample was slowly loaded onto the column, and the flowthrough was collected. Twelve fractions were collected by step eluting with 20  $\mu\text{l}$  each of 40–500 mM NaCl in SAX buffer. Flowthrough and eluate fractions were briefly concentrated in a speedvac to reduce the acetonitrile concentration, brought to 5% formic acid, and desalted on R3 microcolumns. IMAC purification of phosphopeptides was done as described above.

## RESULTS AND DISCUSSION

Freshly isolated plant plasma membranes are mostly right side-out, meaning that the cytoplasmic domains of membrane proteins are inside the vesicle. Thus, external ATP cannot be used by the  $\text{H}^+$ -ATPase (Fig. 1A). Johansson *et al.*

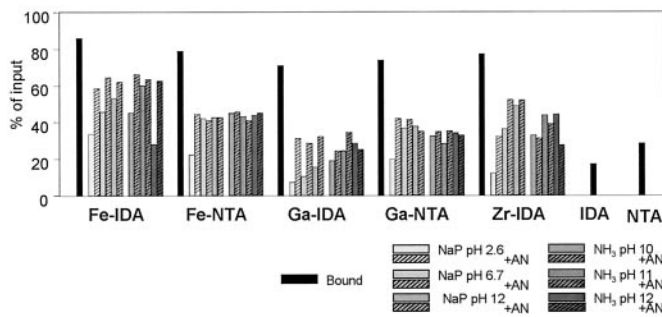


**FIG. 2. Quantitation of phosphopeptides binding to and recovered from different types of IMAC material.** <sup>32</sup>P-labeled phosphopeptides were produced by *in vitro* autophosphorylation of *Arabidopsis* microsomes and purified with the indicated IMAC materials. Phosphate buffer or dilute ammonia with different pH values, with and without addition of 30% acetonitrile, was used for elution. Phosphopeptides were quantified by spotting onto small filter papers and PhosphorImage analysis. “Bound” corresponds to input minus flowthrough. The bars for IDA/NTA indicate unspecific binding to the chelating resins without bound metals.

(33) have shown that low concentrations of the detergent Brij-58 will invert plasma membrane vesicles to nearly 100% inside-out. Similarly, we found that addition of 0.01% Brij-58 to plasma membranes leads to a strong increase in ATP-dependent proton pumping activity (Fig. 1A). After this detergent treatment, the phosphorylated domains of integral membrane proteins should be accessible to protease treatment. To test if differential phosphorylation of plasma membrane proteins in response to microbial elicitors could be detected at the peptide level, we isolated plasma membranes from cells labeled with [<sup>32</sup>P]orthophosphate *in vivo* before or after elicitation with flg22, inverted with 0.01% Brij-58, digested with trypsin, and used IMAC to enrich for phosphopeptides. The PhosphorImages of two-dimensional thin-layer chromatography (TLC)-thin-layer electrophoresis (TLE) analysis shows multiple changes in response to the microbial elicitor flg22 (Fig. 1B). A number of the radioactive peptides are equally present in both samples, indicating that the differences are a result of the biological response and not from losses during sample handling. We therefore decided to develop this membrane-“shaving” approach with the ultimate goal of detecting plasma membrane-based signaling events triggered by elicitors.

There are two concerns about the use of IMAC: On the one hand, not all phosphopeptides bind to IMAC resins (34); on the other, the fraction eluted from IMAC is allegedly strongly contaminated with (particularly acidic) nonphosphorylated peptides (10). Despite these concerns, no study has clearly demonstrated what percentage of phosphopeptides is recovered from a complex mixture by IMAC. We have produced <sup>32</sup>P-radiolabeled phosphopeptides by *in vitro* autophosphorylation of microsomal membranes and quantitatively determined the amount of phosphopeptides bound to and released from various types of IMAC materials. Two chelating resins, iminodiacetic acid (IDA) on POROS MC beads (35) and NTA

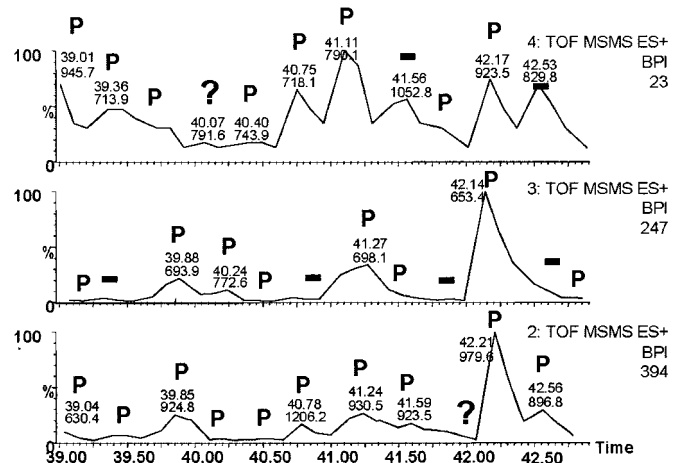


**FIG. 3. Purity of batch-IMAC isolated phosphopeptides by Q-TOF LC-MS/MS analysis.** A plasma membrane digest (100 μg plasma membrane protein) was batch-incubated with Fe<sup>3+</sup>-NTA, and peptides eluted with 50 mM ammonium phosphate were analyzed by LC-MS/MS on a Q-TOF instrument. Total ion currents for the three MS/MS cycles (see “Materials and Methods”) are shown; the elution of phosphopeptides (judged by neutral loss of H<sub>3</sub>PO<sub>4</sub>, Δm = 98 Da) and nonphosphorylated peptides are marked with “P” and “-,” respectively.

on silica (12), were loaded with Fe<sup>3+</sup> (31), Ga<sup>3+</sup>, ZrO<sup>2+</sup>, Sc<sup>3+</sup> (35), Cu<sup>2+</sup>, and Zn<sup>2+</sup>. For convenience, the peptides were batch-incubated with the IMAC resin for 5 min and then loaded into a microcolumn to wash out unbound peptides. For elution from IMAC resins, either potassium phosphate buffers at various pHs or dilutions of ammonia in ddH<sub>2</sub>O were used, both with and without 30% added acetonitrile.

About 80% of the radioactivity bound to almost any immobilized metal, but the binding was nearly irreversible in the case of Cu<sup>2+</sup> and Zn<sup>2+</sup> (data not shown). Capture and release were most efficient with Fe<sup>3+</sup>-IDA resin using phosphate or base elution, followed by ZrO<sup>2+</sup>-IDA and Fe<sup>3+</sup>-NTA (Fig. 2). Both chelating resins bound 20–30% of the phosphopeptides unspecifically and, for the duration of the washes, “irreversibly” even without bound metal. From these results, Fe<sup>3+</sup>-IDA (POROS MC) was chosen for all further experiments, with base elution for subsequent phosphatase treatment or phosphate elution for direct desalting and MS analysis.

Our quantitative results differ considerably from those of Posewitz and Tempst (35), especially for the recovery of phosphopeptides from Fe<sup>3+</sup>-IDA with aqueous ammonia. We think that the difference is mainly due to the different aims in phosphopeptide capture MALDI compatibility (35) *versus* preparative-scale isolation in our study. We have eluted the peptides with a larger volume of dilute ammonia to achieve a sufficiently high pH in the column, and left the column for at least 5 min in these alkaline conditions (see “Materials and Methods”). Posewitz and Tempst note that with their eluting conditions, the eluate was “mildly alkaline,” suggesting that their Fe<sup>3+</sup>-IMAC columns may not have reached the original pH of the eluant. They further note that “more than 10 vol-

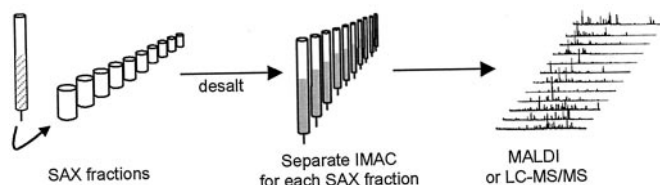


FIG. 4. **Scheme of two-dimensional LC separation.** Total plasma membrane digests (500  $\mu\text{g}$  plasma membrane protein) were fractionated by SAX chromatography. Ten to 15 step-eluted fractions were desalted and individually incubated with IMAC resin. Peptides eluted from IMAC were then analyzed by MALDI or LC-MS/MS.

umes of the elution solvent, or significantly lower flow rate, was required to even begin desorbing the phosphorylated peptides.” Our conditions are closer to this description. The recovery of 60–70% of the input is lower than previously reported for synthetic peptides (35) but is perhaps more meaningful as it represents a mixed population of peptides. This figure likely comprises both a random loss from incomplete recovery of most peptides and a sequence-dependent loss of specific subpopulations. Therefore, 70% coverage of the total phosphoproteome is a minimal estimate. In addition, the use of proteases other than trypsin should further improve coverage, as has been shown for elastase digestion combined with IMAC (36).

We isolated a phosphopeptide-enriched fraction from “shavings” of 100  $\mu\text{g}$  plasma membrane protein and used capillary LC-MS/MS to analyze what fraction of the peptides is phosphorylated. Fig. 3 shows a 3-min section of LC-MS/MS ion chromatogram traces from three channels. Phosphopeptides can easily be recognized by one or multiple neutral losses of phosphoric acid during mass spectrometry resulting in the appearance of satellite peaks with a mass 98 Da (and multiples thereof) lower than the parent ion mass (data not shown). The satellite peaks appear in the MS/MS spectra and sometimes, without collision-induced dissociation, in the original MS trace. Both cases have been marked with “P” in the ion trace (Fig. 3). Of 20 peptides automatically submitted to MS/MS analysis (annotated with elution time and  $m/z$ ), 17 were phosphopeptides. When the minor signals are included, about 75% of all peptides eluting in the analyzed time window show neutral loss of phosphoric acid and thus are phosphopeptides. As the purity of the IMAC eluate is not absolute, enrichment by IMAC is no proof that a peptide is a phosphopeptide. It is immediately obvious, however, that the enrichment virtually eliminated the problem of suppression of phosphopeptide signals by nonphosphorylated peptides. We would like to emphasize that this level of purity was achieved with unmodified peptides. A recent pioneering large-scale phosphoproteomic study (10) observed that IMAC purification only yielded phosphopeptides with sufficient purity if the peptides were carboxy-methylated, thus eliminating nonspecific binding by acidic peptides. We feel that this problem is generally overestimated, but cannot exclude that the type of

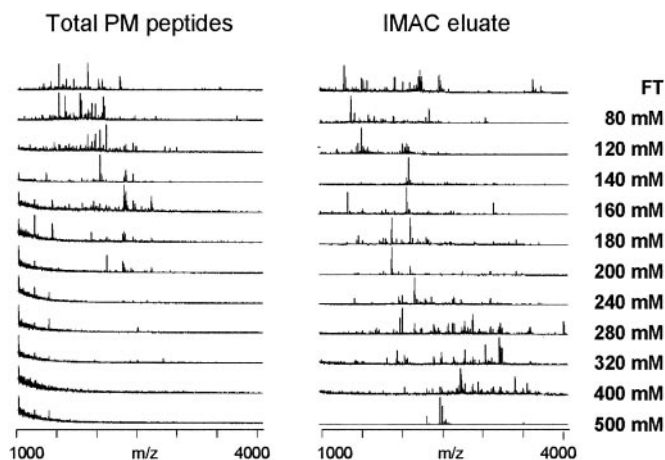
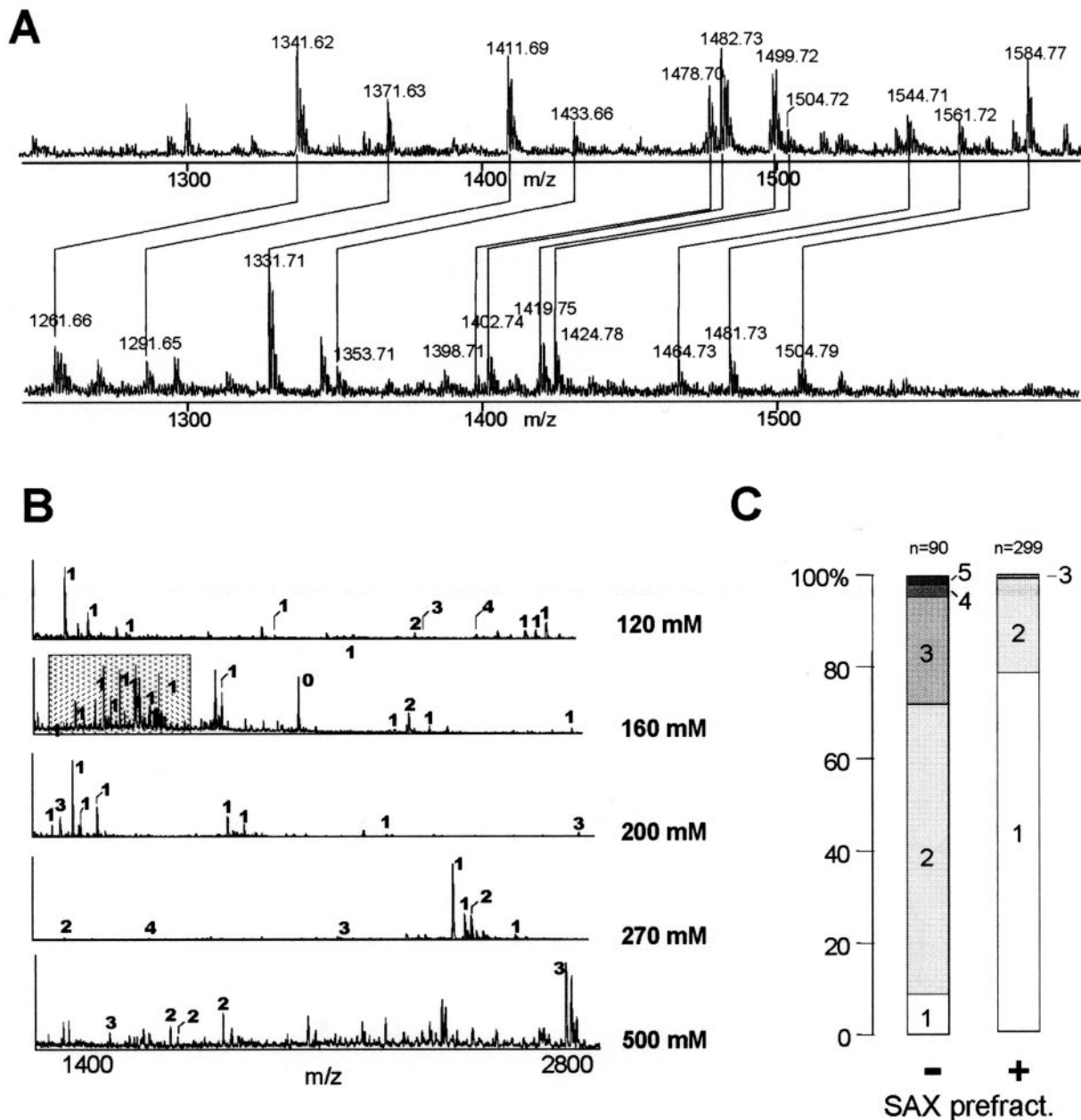


FIG. 5. **Elution profile of total peptides and phosphopeptides from SAX.** Aliquots of the original SAX fractions (*Total PM peptides*) and the IMAC-purified peptides isolated from those fractions (*IMAC eluate*) were analyzed by MALDI. FT denotes unbound material; elution steps (NaCl concentration) are indicated.

sample used in our study, plant plasma membranes, is more conducive to a straightforward approach with native phosphopeptides. A closer investigation of the type of contaminating peptides is shown further below.

The initial results with batch-IMAC purification were very encouraging but also showed two limitations. First, among the identified peptides (see supplementary Table I for a representative experiment), those with two and more phosphorylation sites were far more abundant than those with one. Ficarro *et al.* (10) made the same observation and suggested that multiphosphorylated peptides bind more strongly to the affinity resin, thus outcompeting the singly phosphorylated ones. Adjusting the sample/resin ratio should solve the problem, but may also bring a penalty in yield and purity. Second, the batch-purified plasma membrane phosphopeptide sample is an extremely complex mixture. The Q-TOF mass spectrometer was operating at the upper limit of LC-MS/MS data acquisition in automatic mode and, as is typical for large-scale analyses, only skimmed the most abundant peptides. No proteomic study can reliably estimate the number of undetected rare proteins/peptides, and full coverage is probably impossible to achieve. Nevertheless, an additional analytical dimension by pre-IMAC fractionation of the peptide mix would be necessary to overcome the acquisition limitations in the MS-MS/MS cycle of the instrument.

The most typical and successful combination of chromatographic separations of peptides consists of a strong cation exchanger (SCX) followed by reversed-phase chromatography, the latter typically coupled online to MS (37). SCX is performed under strongly acidic conditions where peptides are fully protonated. The  $pK$  values of phosphoamino acid residues, however, are much lower than those of glutamic and aspartic acid, and phosphopeptides retain negative charges under SCX conditions. We found the binding of phosphopep-



**FIG. 6. Elution of mono- and multiphosphorylated peptides from the SAX column.** *A*, comparison of IMAC-purified peptides from the 160 mM NaCl SAX fraction before (*top*) and after (*bottom*) dephosphorylation. *B*, phosphopeptide signals in the MALDI spectra of IMAC eluates (see Fig. 5, *right panel*; NaCl concentration steps indicated) were annotated with the number of phosphate groups (where possible) by comparing the spectra before and after dephosphorylation with alkaline phosphatase. Signals with unchanged mass after dephosphorylation are marked "0"; unmarked peaks were ambiguous. The *shaded box* indicates the part of the spectrum that is shown enlarged in *A*. *C*, percentage of singly and multiply phosphorylated peptides (not including contaminants) in IMAC eluates. *Left* (-), one-step batch isolation (cumulative of several independent experiments with 100  $\mu$ g protein each; total 90 phosphopeptides). *Right* (+), cumulative of several experiments with 10–12 SAX fractions using 500  $\mu$ g starting material (total 299 phosphopeptides).

tides to cation exchange resin rather poor (data not shown). It seemed logical to try a strong anion exchange material instead, which is for technical reasons not generally used for peptides (37) but seemed appropriate for (poly)anionic phosphopeptides. Fig. 4 shows the strategy we used. The crude peptide mixture obtained by membrane digestion was frac-

tionated by SAX. Ten to 15 fractions were desalted by reversed-phase chromatography on POROS Oligo<sup>TM</sup>-R3 microcolumns (38) and batch-incubated with Fe<sup>3+</sup>-IDA (POROS MC). Peptides eluted from IMAC were analyzed by either MALDI MS or LC-MS/MS. Fig. 5 shows that the majority of all peptides eluted from SAX between 0 and 150 mM salt,

whereas phosphopeptides eluted over a much wider range (0–500 mM). These results confirm that SAX is suitable as a pre-fractionation step before IMAC.

We routinely monitored the efficiency of phosphopeptide enrichment by comparing MALDI spectra of original and dephosphorylated IMAC eluates. While screening the SAX-pre-fractionated and IMAC-purified peptides, we noticed that fractions eluting from the SAX column at low salt contained an abundance of singly phosphorylated peptides (Fig. 6A). This was in stark contrast to the small number of monophosphorylated peptides recovered in batch-binding experiments. As expected for polyanions, multiphosphorylated peptides were more strongly retained by SAX and eluted at higher salt concentrations (Fig. 6B). This result suggests that SAX pre-fractionation not only allows a better coverage of the total phosphoproteome by virtue of the two-dimensional separation, but also presents a solution to the bias against singly phosphorylated peptides mentioned earlier. We think that the incubation of each SAX-eluted fraction *separately* with IMAC (as opposed to a two-dimensional LC separation of peptides eluting from IMAC) is essential for the recovery of monophosphorylated peptides from highly complex mixtures.

We decided to do a preparative isolation of PM peptides (500  $\mu$ g plasma membrane protein) and analyze each IMAC eluate (as described in Fig. 4) with LC-MS/MS for a large-scale experiment. Twelve SAX fractions including the flowthrough were analyzed. Representative data from both the batch-isolation and SAX pre-fractionation are shown in supplementary Table I (an in-depth analysis of the phosphorylation sites and their biological relevance will be presented elsewhere). From 320 peptides with significant Mascot scores, 299 were phosphopeptides, indicating >90% purity. This level of purity represents a substantial improvement over the batch binding experiment. Importantly, however, monophosphorylated peptides now represented 78%, rather than 9%, of the identified phosphopeptides (Fig. 6C). A preliminary survey showed that many phosphoproteins were missed in the earlier experiment with total batch-IMAC. On the other hand, few triply or higher phosphorylated peptides were found in the large-scale study, possibly because of the reverse-phase purification before and after SAX. Some multiphosphorylated peptides do not either bind to or elute from the reverse-phase column efficiently (38). We do, however, see several polyphosphorylated peptides by MALDI (Fig. 6B) and suspect that most of them yield fragmentation spectra of too low quality to be identified by MASCOT. In addition, the high-salt eluates contain very low peptide concentrations (compare Fig. 5, *left panels*), and adsorptive loss of peptides may be more pronounced. Taken together, one-step batch IMAC and our novel two-dimensional LC fractionation are complementary for coverage of both singly and multiply phosphorylated peptides in large-scale phosphoproteomics.

It has often been stated (1, 10, 39) that acidic peptides are the major reason for unsatisfactory specificity of IMAC purifi-

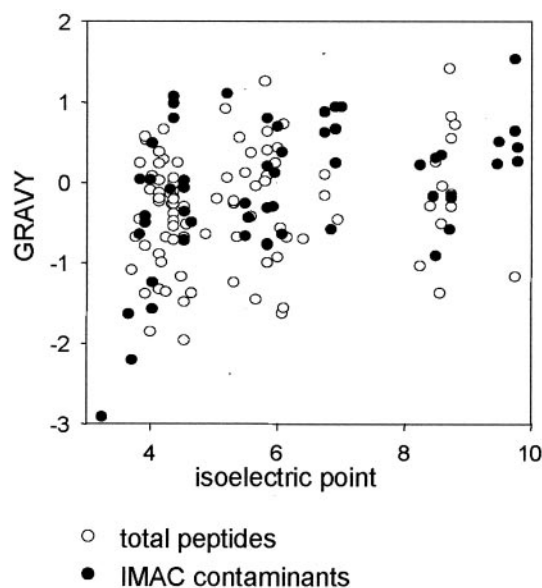


Fig. 7. Physicochemical properties of nonphosphorylated (contaminant) peptides found in IMAC eluates compared with those of total plasma membrane peptides. Isoelectric points and grand average hydrophobicity (GRAVY) were calculated with the ProtParam tool (ca.expasy.org/tools/protparam.html). The parameter pairs were plotted for all 65 nonphosphorylated peptides from the large-scale SAX fractionation (IMAC contaminants, ●) as well as for 100 randomly chosen peptides identified in an LC-MS/MS run of a crude plasma membrane digest (total peptides, ○).

cations. We have taken all sequences of nonphosphorylated peptides that eluted from IMAC (from several batch binding and pre-fractionation experiments) and compared the physical properties of these 65 contaminant peptides with those of 100 random peptides identified in an LC-MS/MS run of total plasma membrane “shavings” (data not shown). As shown in Fig. 7, the distribution of hydrophobicity and isoelectric points in the nonphosphorylated IMAC “contaminants” is not significantly different from that of total plasma membrane peptides. Specifically, they neither have a more acidic pI nor do they contain more clustered glutamic and aspartic acid residues (data not shown). Rather, a large number of contaminant peptides came from proteins that were identified with a high score in the analysis of total peptides, indicating that they represent the most abundant proteins in the membrane. From these results, we argue that concerns of acidic contaminants are overstated for the IMAC enrichment of phosphopeptides from complex peptide mixtures. As stated above, we cannot rule out that plasma membranes are particularly unproblematic, but initial experiments with total soluble protein digests show similar purity of 70–80% phosphopeptides (data not shown).

As an example of the novel phosphorylation sites found in this study, Fig. 8 lists all identified phosphopeptides from isoforms of the plasma membrane H<sup>+</sup>-ATPase. P-type ATPases generate the electrochemical proton gradient across the plasma membrane in plants and fungi (40). Various stimuli

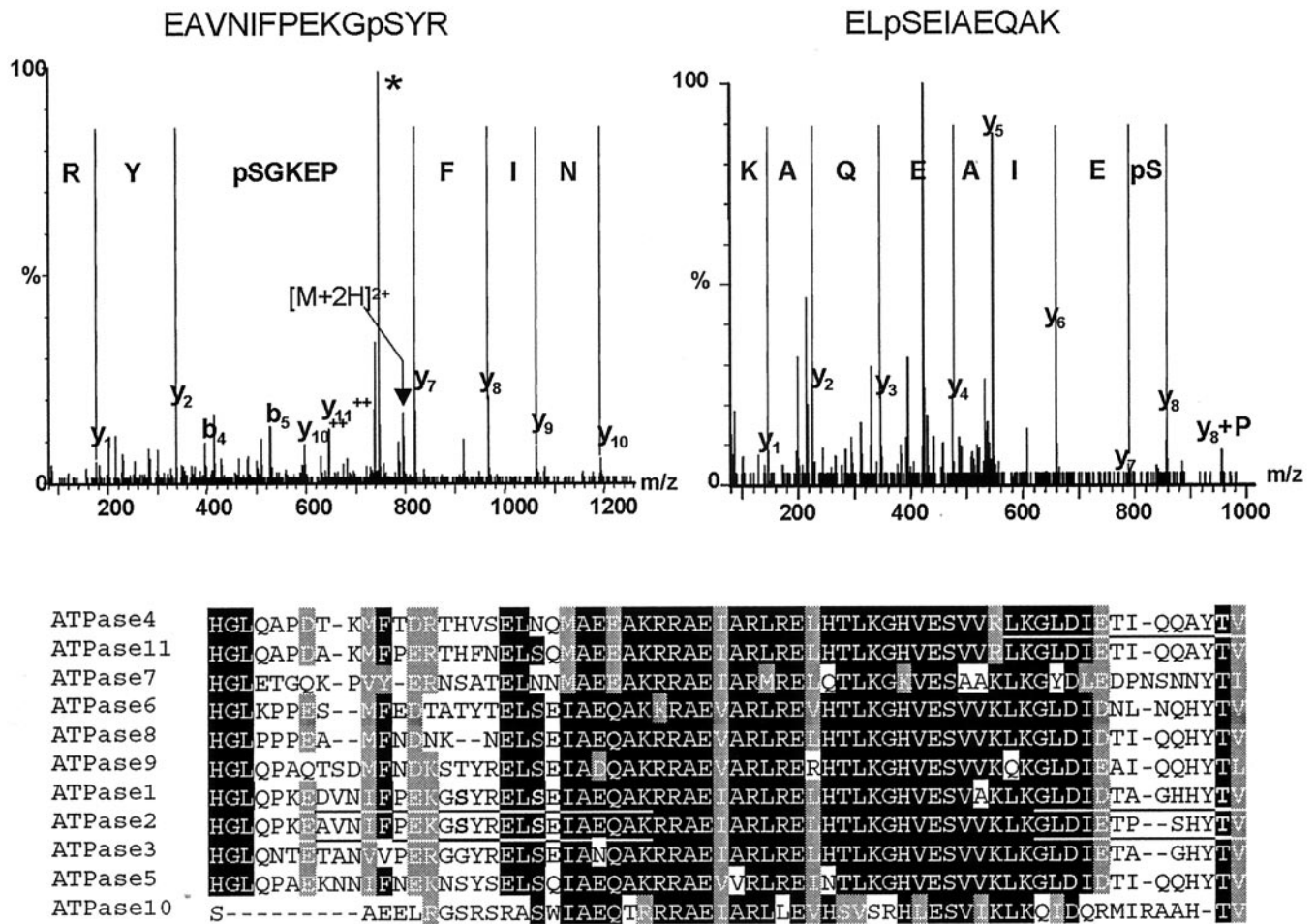


Fig. 8. **Novel phosphorylation sites on H<sup>+</sup>-ATPase proteins.** *Top*, MS/MS spectra for the phosphopeptides E<sup>889</sup>AVNIFPEKGpSYR<sup>901</sup> of ATPase 2 (At4g30190) and ELpSEIAEQAK (conserved between ATPase 1 (At2g18960) and ATPase 2). *Bottom*, ClustalW analysis of the C termini of ATPase isoforms 1–11 of *Arabidopsis*. The identified phosphopeptides are *underlined* and phosphorylated residues printed in *bold*. The peptide ELpSEIAEQAK comes from either AHA1 or AHA2; the peptide LKGLDIETIQQAYTV from either AHA4 or AHA11.

are known to regulate H<sup>+</sup>-ATPases in plants. For example, blue light stimulates proton pumping in guard cells (41), and deactivation occurs in response to the wounding peptide hormone, systemin (42). It is likely that H<sup>+</sup>-ATPase deactivation also contributes to the very rapid medium alkalinization observed in elicitor-treated cell cultures (43), which would make the ATPase(s) one of the earliest targets of microbial elicitor-induced signal transduction.

Regulation of plant plasma membrane ATPases through phosphorylation is well documented, although whether phosphorylation or dephosphorylation activates the enzyme is controversial and appears to depend on the experimental conditions. *In vitro*, the plant H<sup>+</sup>-ATPase can be phosphorylated by a plasma membrane-resident calcium-dependent protein kinase (44, 45). The conserved penultimate threonine residue (Thr947 of AHA2) is so far the only known *in vivo* phosphorylation site (14). Binding of a 14-3-3 protein to the noncanonical phosphorylated motif generates a target for the fungal toxin fusicoccin (46), which results in nearly irreversible

activation of the proton pump. It is likely that multiple kinases regulate the enzyme at different sites, some with opposite effects on enzyme activity. Clearly, it is essential to identify *in vivo* phosphorylation sites in addition to the penultimate threonine residue. We have found the c-terminal phosphopeptide from three AHA isoforms. In addition, we discovered two novel sites on AHA1/AHA2 (Fig. 8). Both sites are close to the postulated regulatory R1 region of the C terminus (47).

#### CONCLUSION

We have established a simple and robust strategy for the large-scale identification of phosphorylation sites. The enrichment of phosphopeptides from crude, complex mixtures by IMAC is more efficient than generally assumed and yields a preparation that is suitable for direct LC-MS/MS analysis. We have successfully extended the “shaving” approach for membrane proteomics—analyzing peptides rather than whole proteins—to phosphoproteomics. Applying the strategy to plasma membranes of *Arabidopsis*, and incorporating a novel



two-dimensional LC separation, we have found over 200 phosphopeptides, among them two previously unknown phosphorylation sites on isoforms of the proton ATPase. Although further work is necessary to establish biological functions and dynamics of the identified sites, as well as to improve coverage of the phosphoproteome, such large-scale data overcome a major bottleneck in signaling research because *in vivo* phosphorylation sites of low-abundance membrane proteins are exceedingly difficult to identify by classical approaches. We expect that the presented simple IMAC method can be applied with minor modifications to study other organelles and soluble proteins. In addition, our approach can be extended to study the dynamics of protein phosphorylation by introducing stable isotopes into the proteins/peptides through metabolic labeling (48), during the digest (49), or by post-digest chemical labeling (50) for quantitative mass spectrometry.

\* This work was supported by Biotechnology and Biological Sciences Research Council Grant 83/C17990 (to T. S. N. and S. C. P.), the Gatsby Charitable Foundation (to T. S. N. and S. C. P.), a grant from the Danish Natural Sciences Research Council (to O. N. J.), an EMBO Short-Term fellowship (to T. S. N.), and a Danish Industrial PhD fellowship (to A. S.). The costs of publication of this article were defrayed in part by the payment of page charges. This article must therefore be hereby marked "advertisement" in accordance with 18 U.S.C. Section 1734 solely to indicate this fact.

¶ To whom correspondence should be addressed: Scott Peck, The Sainsbury Laboratory, John Innes Centre, Colney Lane, Norwich NR4 7UH, United Kingdom. Fax: 44-(0)1603-450011; E-mail: scott.peck@sainsbury-laboratory.ac.uk. Ole Nørregaard Jensen, Department of Biochemistry and Molecular Biology, University of Southern Denmark, DK-5230 Odense M, Denmark. Fax: 45-6550-2467; E-mail: jenseno@bmb.sdu.dk.

REFERENCES

1. Mann, M., Ong, S. E., Gronborg, M., Steen, H., Jensen, O. N., and Pandey, A. (2002) Analysis of protein phosphorylation using mass spectrometry: Deciphering the phosphoproteome. *Trends Biotechnol.* **20**, 261–268
2. Cohen, P. (2000) The regulation of protein function by multisite phosphorylation—A 25 year update. *Trends Biochem. Sci.* **25**, 596–601
3. Maguire, P. B., Wynne, K. J., Harney, D. F., O'Donoghue, N. M., Stephens, G., and Fitzgerald, D. J. (2002) Identification of the phosphotyrosine proteome from thrombin activated platelets. *Proteomics*, **2**, 642–648
4. Steen, H., Kuster, B., Fernandez, M., Pandey, A., and Mann, M. (2002) Tyrosine phosphorylation mapping of the epidermal growth factor receptor signaling pathway. *J. Biol. Chem.* **277**, 1031–1039
5. Kim, H. J., Song, E. J., and Lee, K. J. (2002) Proteomic analysis of protein phosphorylations in heat shock response and thermotolerance. *J. Biol. Chem.* **277**, 23193–23207
6. Gronborg, M., Kristiansen, T. Z., Stensballe, A., Andersen, J. S., Ohara, O., Mann, M., Jensen, O. N., and Pandey, A. (2002) A mass spectrometry-based proteomic approach for identification of serine/threonine-phosphorylated proteins by enrichment with phospho-specific antibodies: Identification of a novel protein, Frigg, as a protein kinase A substrate. *Mol. Cell. Proteomics* **1**, 517–527
7. Oda, Y., Nagasu, T., and Chait, B. T. (2001) Enrichment analysis of phosphorylated proteins as a tool for probing the phosphoproteome. *Nat. Biotechnol.* **19**, 379–382
8. Zhou, H. L., Watts, J. D., and Aebersold, R. (2001) A systematic approach to the analysis of protein phosphorylation. *Nat. Biotechnol.* **19**, 375–378
9. Salomon, A. R., Ficarro, S. B., Brill, L. M., Brinker, A., Phung, Q. T., Ericson, C., Sauer, K., Brock, A., Horn, D. M., Schultz, P. G., and Peters, E. C. (1–21-2003) Profiling of tyrosine phosphorylation pathways in human

- cells using mass spectrometry. *Proc. Natl. Acad. Sci. U. S. A.* **100**, 443–448
10. Ficarro, S. B., McClelland, M. L., Stukenberg, P. T., Burke, D. J., Ross, M. M., Shabanowitz, J., Hunt, D. F., and White, F. M. (2002) Phosphoproteome analysis by mass spectrometry and its application to *Saccharomyces cerevisiae*. *Nat. Biotechnol.* **20**, 301–305
11. Vener, A. V., Harms, A., Sussman, M. R., and Vierstra, R. D. (2001) Mass spectrometric resolution of reversible protein phosphorylation in photosynthetic membranes of *Arabidopsis thaliana*. *J. Biol. Chem.* **276**, 6959–6966
12. Stensballe, A., Andersen, S., and Jensen, O. N. (2001) Characterization of phosphoproteins from electrophoretic gels by nanoscale Fe(III) affinity chromatography with off-line mass spectrometry analysis. *Proteomics* **1**, 207–222
13. Porath, J., Carlsson, J., Olsson, I., and Belfrage, G. (1975) Metal chelate affinity chromatography, a new approach to protein fractionation. *Nature* **258**, 598–599
14. Fuglsang, A. T., Visconti, S., Drumm, K., Jahn, T., Stensballe, A., Mattei, B., Jensen, O. N., Aducci, P., and Palmgren, M. G. (1999) Binding of 14-3-3 protein to the plasma membrane H(+)-ATPase AHA2 involves the three C-terminal residues Tyr(946)-Thr-Val and requires phosphorylation of Thr(947). *J. Biol. Chem.* **274**, 36774–36780
15. Torres, M. A., Dangl, J. L., and Jones, J. D. (2002) Arabidopsis gp91phox homologues AtrbohD and AtrbohF are required for accumulation of reactive oxygen intermediates in the plant defense response. *Proc. Natl. Acad. Sci. U. S. A.* **99**, 517–522
16. Mellersh, D. G., and Heath, M. C. (2001) Plasma membrane-cell wall adhesion is required for expression of plant defense responses during fungal penetration. *Plant Cell* **13**, 413–424
17. Nimchuk, Z., Marois, E., Kjemtrup, S., Leister, R. T., Katagiri, F., and Dangl, J. L. (2000) Eukaryotic fatty acylation drives plasma membrane targeting and enhances function of several type III effector proteins from *Pseudomonas syringae*. *Cell* **101**, 353–363
18. Romeis, T., Piedras, P., and Jones, J. D. (2000) Resistance gene-dependent activation of a calcium-dependent protein kinase in the plant defense response. *Plant Cell* **12**, 803–816
19. Lebrun-Garcia, A., Bourque, S., Binet, M. N., Ouaked, F., Wendehenne, D., Chiltz, A., Schaffner, A., and Pugin, A. (1999) Involvement of plasma membrane proteins in plant defense responses. Analysis of the cryptogeiin signal transduction in tobacco. *Biochimie (Paris)* **81**, 663–668
20. Blumwald, E., Aharon, G. S., and Lam, B. C-H. (1998) Early signal transduction pathways in plant-pathogen interactions. *Trends Plant Sci.* **3**, 342–346
21. Peck, S. C., Nuhse, T. S., Hess, D., Iglesias, A., Meins, F., and Boller, T. (2001) Directed proteomics identifies a plant-specific protein rapidly phosphorylated in response to bacterial and fungal elicitors. *Plant Cell* **13**, 1467–1475
22. Wu, C. C., and Yates, J. R. (2003) The application of mass spectrometry to membrane proteomics. *Nat. Biotechnol.* **21**, 262–267
23. Han, D. K., Eng, J., Zhou, H., and Aebersold, R. (2001) Quantitative profiling of differentiation-induced microsomal proteins using isotope-coded affinity tags and mass spectrometry. *Nat. Biotechnol.* **19**, 946–951
24. Wu, C. C., MacCoss, M. J., Howell, K. E., and Yates, J. R. (2003) A method for the comprehensive proteomic analysis of membrane proteins. *Nat. Biotechnol.* **21**, 532–538
25. Gobom, J., Nordhoff, E., Mirgorodskaya, E., Ekman, R., and Roepstorff, P. (1999) Sample purification and preparation technique based on nanoscale reversed-phase columns for the sensitive analysis of complex peptide mixtures by matrix-assisted laser desorption/ionization mass spectrometry. *J. Mass Spectrom.* **34**, 105–116
26. May, M. J., and Leaver, C. J. (1993) Oxidative stimulation of glutathion synthesis in *Arabidopsis thaliana* suspension cultures. *Plant Physiol.* **103**, 621–627
27. Felix, G., Duran, J. D., Volko, S., and Boller, T. (1999) Plants have a sensitive perception system for the most conserved domain of bacterial flagellin. *Plant J.* **18**, 265–276
28. Nühse, T. S., Peck, S. C., Hirt, H., and Boller, T. (2000) Microbial elicitors induce activation and dual phosphorylation of the *Arabidopsis thaliana* MAPK 6. *J. Biol. Chem.* **275**, 7521–7526
29. Larsson, C., Sommarin, M., and Widell, S. (1994) Isolation of highly purified plant plasma membranes and separation of inside-out and right-side-out

- vesicles. *Methods Enzymol.* **228**, 451–469
30. Palmgren, M. G. (1990) An H<sup>+</sup>-ATPase assay—Proton pumping and ATPase activity determined simultaneously in the same sample. *Plant Physiol.* **94**, 882–886
  31. Andersson, L., and Porath, J. (1986) Isolation of phosphoproteins by immobilized metal (Fe<sup>3+</sup>) affinity chromatography. *Anal. Biochem.* **154**, 250–254
  32. Boyle, W. J., van der Geer, P., and Hunter, T. (1991) Phosphopeptide mapping and phosphoamino acid analysis by two-dimensional separation on thin-layer cellulose plates. *Methods Enzymol.* **201**, 110–149
  33. Johansson, F., Olbe, M., Sommarin, M., and Larsson, C. (1995) Brij 58, a polyoxyethylene acyl ether, creates membrane vesicles of uniform sidedness. A new tool to obtain inside-out (cytoplasmic side-out) plasma membrane vesicles. *Plant J.* **7**, 165–173
  34. Loughrey, Chen S., Huddleston, M. J., Shou, W., Deshaies, R. J., Annan, R. S., and Carr, S. A. (2002) Mass spectrometry-based methods for phosphorylation site mapping of hyperphosphorylated proteins applied to Net1, a regulator of exit from mitosis in yeast. *Mol. Cell. Proteomics* **1**, 186–196
  35. Posewitz, M. C., and Tempst, P. (7–15-1999) Immobilized gallium(III) affinity chromatography of phosphopeptides. *Anal. Chem.* **71**, 2883–2892
  36. Schlosser, A., Bodem, J., Bossemeyer, D., Grummt, I., and Lehmann, W. D. (2002) Identification of protein phosphorylation sites by combination of elastase digestion, immobilized metal affinity chromatography, and quadrupole-time of flight tandem mass spectrometry. *Proteomics* **2**, 911–918
  37. Link, A. J. (2002) Multidimensional peptide separations in proteomics. *Trends Biotechnol.* **20**, S8–13
  38. Neubauer, G., and Mann, M. (1999) Mapping of phosphorylation sites of gel-isolated proteins by nano-electrospray tandem mass spectrometry: Potentials and limitations. *Anal. Chem.* **71**, 235–242
  39. Kalume, D. E., Molina, H., and Pandey, A. (2003) Tackling the phosphoproteome: Tools and strategies. *Curr. Opin. Chem. Biol.* **7**, 64–69
  40. Palmgren, M. G. (2001) Plant plasma membrane H<sup>+</sup>-ATPases: Powerhouses for nutrient uptake. *Annu. Rev. Plant Physiol. Plant Mol. Biol.* **52**, 817–845
  41. Kinoshita, T., and Shimazaki, K. (1999) Blue light activates the plasma membrane H<sup>+</sup>-ATPase by phosphorylation of the C-terminus in stomatal guard cells. *EMBO J.* **18**, 5548–5558
  42. Schaller, A., and Oecking, C. (1999) Modulation of plasma membrane H<sup>+</sup>-ATPase activity differentially activates wound and pathogen defense responses in tomato plants. *Plant Cell* **11**, 263–272
  43. Mathieu, Y., Lapous, D., Thomine, S., Lauriere, C., and Guern, J. (1996) Cytoplasmic acidification as an early phosphorylation-dependent response of tobacco cells to elicitors. *Planta* **199**, 416–424
  44. Lino, B., Baizabal-Aguirre, V. M., and Gonzalez de la Vara LE (1998) The plasma-membrane H<sup>+</sup>-ATPase from beet root is inhibited by a calcium-dependent phosphorylation. *Planta* **204**, 352–359
  45. Schaller, G. E., and Sussman, M. R. (1988) Phosphorylation of the plasma-membrane H<sup>+</sup>-ATPase of oat roots by a calcium-stimulated protein kinase. *Planta* **173**, 509–518
  46. Wurtele, M., Jelich-Ottmann, C., Wittinghofer, A., and Oecking, C. (2003) Structural view of a fungal toxin acting on a 14-3-3 regulatory complex. *EMBO J.* **22**, 987–994
  47. Axelsen, K. B., Venema, K., Jahn, T., Baunsgaard, L., and Palmgren, M. G. (1999) Molecular dissection of the C-terminal regulatory domain of the plant plasma membrane H<sup>+</sup>-ATPase AHA2: Mapping of residues that when altered give rise to an activated enzyme. *Biochemistry* **38**, 7227–7234
  48. Ong, S. E., Blagoev, B., Kratchmarova, I., Kristensen, D. B., Steen, H., Pandey, A., and Mann, M. (2002) Stable isotope labeling by amino acids in cell culture, SILAC, as a simple and accurate approach to expression proteomics. *Mol. Cell. Proteomics* **1**, 376–386
  49. Bonenfant, D., Schmelzle, T., Jacinto, E., Crespo, J. L., Mini, T., Hall, M. N., and Jenoe, P. (2003) Quantitation of changes in protein phosphorylation: A simple method based on stable isotope labeling and mass spectrometry. *Proc. Natl. Acad. Sci. U. S. A.* **100**, 880–885
  50. Tao, W. A., and Aebersold, R. (2003) Advances in quantitative proteomics via stable isotope tagging and mass spectrometry. *Curr. Opin. Biotechnol.* **14**, 110–118